Mem. S.A.It. Vol. 76, 309

Memorie della

Brown dwarf circumstellar disk structure

C. Walker[1], K. Wood[1], C. J. Lada[2], T. Robitaille[1], J.E. Bjorkman[3] and B. Whitney[4]

[1] School of Physics & Astronomy, University of St. Andrews, North Haugh, St Andrews, KY16 9SS, Scotland e-mail: cw26@st-and.ac.uk
[2] Harvard-Smithsonian Center for Astrophysics, 60 Garden Street, Cambridge, MA 02138
[3] Ritter Observatory, Department of Physics & Astronomy, University of Toledo, Toledo, OH 43606
[4] Space Science Institute, 3100 Marine Street, Suite A353, Boulder, CO 80303

Abstract. We present synthetic spectra for circumstellar disks that are heated by radiation from a central brown dwarf. Under the assumption of vertical hydrostatic equilibrium, our models yield scaleheights for brown dwarf disks in excess of three times those derived for classical T Tauri (CTTS) disks. Such highly flared disks around brown dwarfs will result in a large fraction of obscured sources due to extinction of direct starlight by the disk over a wide range of sightlines This could impact on the optical and near-IR detectability of such systems.

Key words. Circumstellar Disks – Brown Dwarfs – Radiation Transfer Models

1. Introduction

Accumulating observational evidence indicates the presence of circumstellar disks around brown dwarfs, including near-IR (e.g., Muench et al. 2001; Liu et al. 2003) and mid-IR excess emission (Comerón et al. 1998; 2000). The discovery of circumstellar disks around brown dwarfs is important as it could suggest that they form in a similar fashion to more massive T Tauri stars (Shu, Adams, & Lizano 1987). Data indicating significant masses and extents of circumstellar material may also cause problems for brown dwarf formation scenarios involving ejection (Reipurth & Clarke 2001).

Brown dwarfs have previously been modelled using flat and flared reprocessing disks (e.g., Natta & Testi 2001; Liu et al. 2003).

2. Model Ingredients

This study was carried out using a Monte Carlo radiation transfer code that is described by Walker et al. (2004) and references therein. We self-consistently determine the density structure of a passive disk in vertical hydrostatic equilibrium with dust and gas well mixed throughout the disk.

Model disks extend from a dust destruction radius out to 100AU. Within the dust destruction radius we assume there is no material, or material is optically thin. We make the usual thin disk assumptions, assume the disk is non self-gravitating (Pringle 1981) and impose a constant surface density profile $\Sigma \sim \varpi^{-1}$

Send offprint requests to: C. Walker
Correspondence to: School of Physics & Astronomy, North Haugh, St Andrews, KY16 9SS

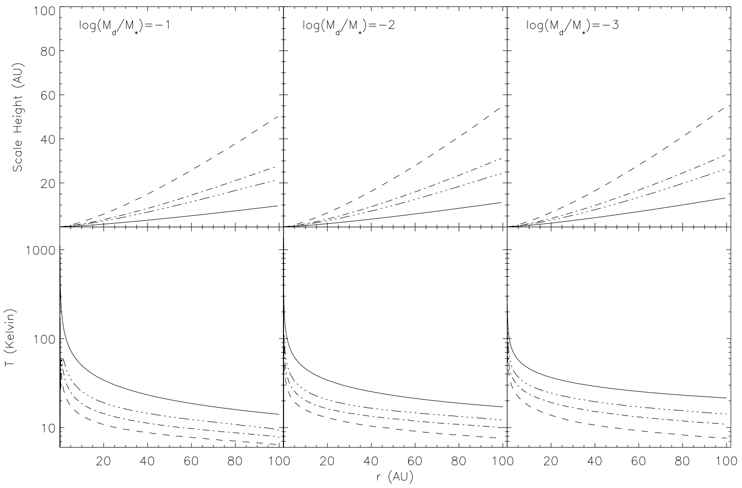

Fig. 1. Upper: Scaleheights of brown dwarf models compared to CTTS models with matching disk mass. Lower: Mid-plane temperatures. In each plot the dashed, dot-dashed and triple dot dashed lines represent central stars of mass $0.01M_\odot$,$0.04M_\odot$ and $0.08M_\odot$ respectively, the solid line represents the CTTS model and mass ratio is indicated in each panel.

Table 1. Model Parameters

$M_\star$ ($M_\odot$)	$T_\star$ (K)	$R_\star$ ($R_\odot$)	$L_\star$ ($L_\odot$)
0.01	2200	0.25	0.0013
0.04	2600	0.50	0.0038
0.08	2800	0.90	0.044

(D'Alessio et al. 1999), where ϖ is the radial coordinate in the disk midplane.

We adopt the dust properties used for modelling of HH 30 IRS (Wood et al. 2002a). Stellar spectra come from BD_Dusty model atmospheres (Allard et al. 2001), with $\log g = 3.5$, and a 4000 K Kurucz model atmosphere (Kurucz 1994).

3. Disk Structure Models

Model parameters are given in Table 1. The stellar masses cover objects from the hydrogen burning limit down to the lower limit for brown dwarfs (Muench et al. 2001). Corresponding radii and temperatures yield models representative of 1Myr old systems (Baraffe et al. 2002). Mass ratios of $\log(M_d/M_\star)$=-1, -2 and -3 are initially considered. Comparisons are made with disks around a typical CTTS with $M_\star = 0.5M_\odot$, $R_\star = 2R_\odot$, and $T_\star = 4000$ K (e.g., D'Alessio et al. 1999).

Figure 1 shows the scaleheights and mid-plane temperatures for our model disks. We calculate the full disk structure, but choose to define scaleheight using the mid-plane temperature. Little variation in mid-plane temperature suggests disk scaleheight is predominantly controlled by stellar mass. CTTS disk scaleheights are in agreement with D'Alessio et al. (1999). The brown dwarf disks have h(100 AU) ranging from just over 20 AU for $M_\star = 0.08M_\odot$ to almost 60 AU for $M_\star = 0.01M_\odot$.

4. Model Spectra

Figure 2 shows SEDs for our brown dwarf models. Each model has SEDs for ten viewing angles evenly spaced in $\cos i$, so that each curve represents 10% of sources by number assuming sources have random distribution in inclination.

The dependence of SED on disk mass is evident and, as with CTTS, long wavelength ob-

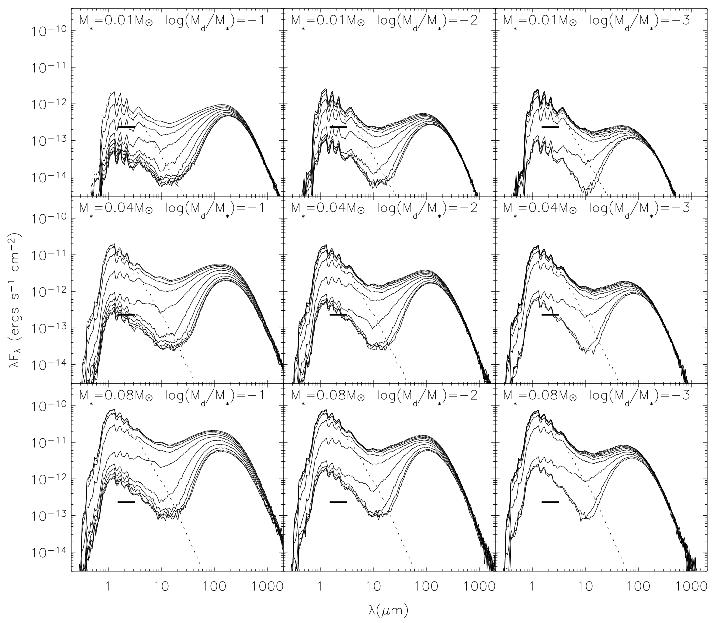

Fig. 2. SEDs for our grid of brown dwarf models. Dotted line is the input stellar spectrum and the solid lines are for ten viewing angles evenly spaced in $\cos i$. The thick horizontal solid line represents a detection limit of 16.5 mags at K.

servations provide the best diagnostics of disk mass. As stellar mass decreases, scaleheights increase allowing the disk to intercept, scatter, and thermally reprocess more stellar radiation, which in turn gives rise to increasingly large IR excesses. Scattered light makes little contribution to face-on models, but it can account for up to 90% of K-band flux as disks become more inclined (see Wood et al. 2002b, Fig. 9).

Compared to CTTS, the larger disk scaleheights we derive for the brown dwarf models will result in a larger fraction of viewing angles over which the central starlight is blocked by the disk. We define an "obscured source" to be one where the near-IR flux is at least three magnitudes fainter than the corresponding face-on source. For CTTS, the obscured fraction is around 20% (D'Alessio et al. 1999; Wood et al. 2002b) for disks of $M_d \sim 10^{-3} M_\odot$.

We find obscured fractions from 20% to 60% with highly inclined sources only detected in the near-IR via scattered light and weak thermal emission. The largest obscured fraction occurs for the lowest stellar mass of $M_\star = 0.01 M_\odot$ with $\log(M_d/M_\star)$=-1 and $T_\star$ = 2200 K. The smallest obscured fraction occurs for the highest stellar mass of $M_\star = 0.08 M_\odot$ with $\log(M_d/M_\star)$=-3 and $T_\star$ = 2800 K.

If the IMF is flat across our mass range then within a young cluster up to 55% of brown dwarf candidates, as defined by our parameter space, may be obscured, using mass ratios of $\log(M_d/M_\star)$=-1. For a declining IMF, and a distribution of disk masses, the obscured fraction will be less.

The relatively low luminosity of brown dwarfs and the increased obscuration due to highly flared disks may present detection problems and, whilst it may be possible to detect some obscured sources, in the absence of high resolution imaging sources may be incorrectly identified as low luminosity systems. CTTS have edge-on flux levels comparable to face-on

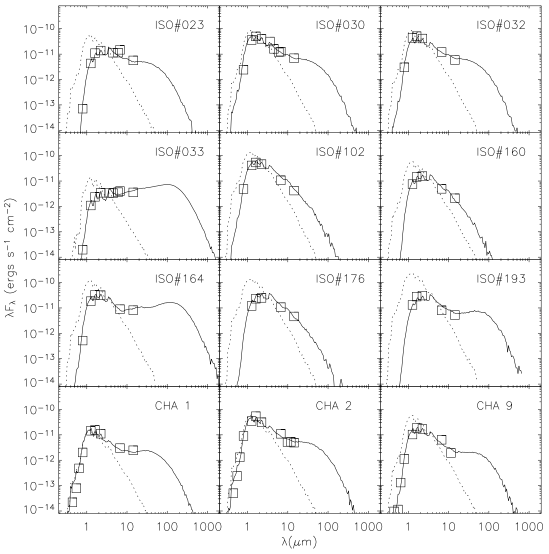

Fig. 3. Models SED fits to observed data in ρ Ophiucus and Chameleon star clusters. Models are of a flared disk with an inner gap of radius $2R_\star$. A distance of 150pc is assumed. Model parameters are given in Walker et al. (2004). The dotted line represents the input spectrum. Models are reddened according to Cardelli, Clayton and Mathis (1989) with $R_v = 4$.

brown dwarfs and similar colors (e.g., Walker et al. 2004).

If brown dwarfs form as a result of ejection from multiple systems then recent numerical simulations by Bate et al. (2003) suggest no disks survive down to their resolution of ~ 10 AU. Therefore, following ejection, disks are expected to be small. We computed SEDs for disks of constant mass, but varying R_d in the range 10AU - 200AU. Because M_d was held constant in these models, smaller R_d yields larger optical depths. The SEDs are mostly unaltered as R_d changes, apart from some variation at far-IR/sub-mm wavelengths. We conclude that it would be very difficult to determine disk radii from SED data alone. High resolution imaging is required to resolve the disks via their scattered light and thermal emission.

5. Comparison to Observations

Figure 3 shows flared disk model fits to the SED data for candidate brown dwarfs in the ρ Ophiucus and Chameleon star clusters.

Table 2. Mass ratios for model fits

Object	$\log(M_d/M_\star)$
ISO#023	-3.6
ISO#030	-3.9
ISO#032	-3.9
ISO#033	-1.0
ISO#102	-5.9
ISO#160	-5.9
ISO#164	-1.9
ISO#176	-5.9
ISO#193	-3.9
CHA Hα1	-3.0
CHA Hα2	-3.6
CHA Hα9	-3.9

Chameleon cluster SED data is taken from Comerón et al (2000) and Apai et al (2002); ρ Ophiucus data comes from Barsony et al. (1997), Comerón et al (1998), Bontemps et al (2001) and Natta et al (2002). Table 2 contains mass ratios for our models and further parameters can be found in Walker et al. (2004). For our model fits we find scaleheights up to three times that of a corresponding CTTS.

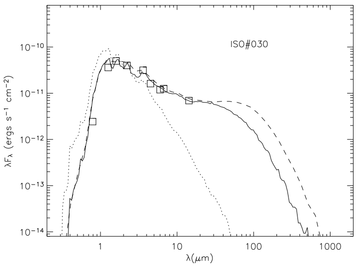

Fig. 4. Two models SED fits as to ISO#030. Solid line indicates surface density $\Sigma \sim \varpi^{-1}$. Dashed line indicates $\Sigma \sim \varpi^{-2}$. The $\Sigma \sim \varpi^{-2}$ model has a disk eight time more massive than the $\Sigma \sim \varpi^{-1}$ case.

Natta & Testi (2001) modelled Cha Hα1, 2, & 9 using a flared disk model. They produced successful fits to the MIR region of the spectrum and predicted a strong 10μm silicate emission feature. Apai et al (2002) later made observations of Cha Hα2 at 9.8 and 11.9 μm and did not detect the silicate feature. They presented an optically thick flat disk model which produced no silicate feature. Natta et al. (2002) found indications that as many as eight of the ρ Oph sources may have flat disks.

As demonstrated by Fig. 3 low mass flared disks can also explain the SEDs previously modelled with flat disks. These models use low mass disks of $10^{-5}M_\odot$ and $10^{-7}M_\odot$ to fit the IR data of the candidates where flat disks were previously suspected. Larger grains naturally suppress the silicate feature [1]. Many of these fits have mass ratios outside the typical range of $-1 \leq log(M_d/M_\star) \leq -3$ (Natta et al. 2000; Klein et al. 2003) and flat disks (Natta et al. 2002) remain a possibility.

Another alternative is that steeper surface density profiles can be used to fit the data with higher mass disks as demonstrated by Fig. 4. Using $\Sigma \sim \varpi^{-2}$ allows us to fit the ISO#030 data with a disk eight times more massive than used in the $\Sigma \sim \varpi^{-1}$ case. Both models fit the data well in the NIR/MIR, but long wavelength observations could discriminate low mass flared disks and steeper surface density disks as well as between these and flat disk models.

If lower mass flared models are representative of disks in brown dwarf populations then problems with obscuration may not be severe. The lower the disk mass, however, the more visible the central source will be (Walker et al. 2004, Fig. 2) and therefore detection via scattered light may only be possible for edge-on systems or using coronographic techniques. Flat disks do not result in severe obscuration of the central star unless at very high inclinations.

6. Summary

We have employed an iterative procedure to determine the hydrostatic density structure of brown dwarf disks. We find brown dwarf disks have large scaleheights, compared to CTTS, due to the lower mass of the central star. In some cases the scaleheights of brown dwarf disks are more than three times larger than for a comparable CTTS system. Larger scaleheights result in more inclinations over which the direct stellar radiation is obscured by the flared disk. The fraction of obscured systems depends on the stellar mass and disk optical depth and in our brown dwarf models is in the range $20\% \leq f_{\rm obs} \leq 60\%$. For a typical CTTS about 20% of sources will be optically obscured.

If brown dwarf disks are highly flared, detection could be biased towards face-on systems. Without direct imaging or spectroscopic identification, it will also be difficult to distinguish between edge-on CTTS and face-on brown dwarfs.

We compare our models to observations of suspected brown dwarfs and show that flared disks of varying mass can account for the observed SEDs and colors. Long wavelength observations are required to discriminate between our flared disk models and alternative flat disk models.

Acknowledgements. Financial support was provided by a UK PPARC studentship (CW) and Advanced Fellowship (KW); NASA's Long Term Space Astrophysics Research Program, NAG5 8412 (BW), NAG5 8794 (JEB); the National Science

[1] New observations of Cha $H\alpha$1 by Sterzik et al. (2004) suggest that small grains may also be required for this source.

Foundation, AST 9909966 (BW), AST 9819928 (JEB).

References

Allard, F., Hauschildt, P.H., Alexander, D.R., Tamanai, A., & Schweitzer, A., 2001, ApJ, 556, 357
Apai, D., Pascucci, I., Henning, Th., Sterzik, M.F., Klein, R., Semenov, D., Gunther, E., & Sterzik, B., 2002, ApJ, 573L, 115
Baraffe, I., Chabrier, G., Allard, F., & Hauschildt, P.H., 2002, A&A, 382, 563
Barsony, M., Kenyon, S.J., Lada, E.A., & Teuban, P.J., 1997, ApJs, 112, 109
Bate, M.R., Bonnell, I.A., & Bromm, V., 2003, MNRAS, 339, 577
Bontemps, S., André, P., & Kaas, A.A., et al., 2001, A&A, 372, 173
Cardelli, J.A., Clayton, G.C., & Mathis, J.S., 1989, 345, 245
Comerón, F., Rieke, G.H., Claes, P., Torra, J., & Laureijs, R.J., 1998, A&A, 335, 522
Comerón, F., Neuhauser, R., & Kaas, A.A., 2000, A&A, 359, 269
D'Alessio, P., Cantó, J., Hartmann, L., Calvet, N., & Lizano, S., 1999, ApJ, 511, 896
Klein, R., Apai, D., Pascucci, I., Henning, Th., & Waters, L.B.F.M., 2003, ApJ, 593, L57
Kurucz, R. L. 1994, CD-ROM 19, Solar Abundance Model Atmospheres (Cambridge: SAO)
Liu, M.C., Najita, J., & Tokunaga, A.T., 2003, ApJ, 585, 372
Muench, A.A., Alves, J., Lada, C.J., & Lada, E.A., 2001, ApJ, 558, 51
Natta, A., Grinin, V.P., & Mannings, V., 2000, in Protostars and Planets IV, ed. V. Mannings, A.Boss, & S.S. Russell (Tucson: Univ. Arizona Press), 559
Natta, A., & Testi, L., 2001, A&A, 376, L22
Natta, A., Testi, L., Comern, F., Oliva, E., D'Antona, F., Baffa, C., Comoretto, G., & Gennari, S., 2002, A&A, 393, 597
Pringle, J.E., 1981, ARA&A, 19, 137
Reipurth, B., & Clarke, C., 2001, AJ, 122, 432
Shakura, N.I., & Sunyaev, R.A., 1973, A&A, 24, 337
Shu, F.H., Adams, F.C., & Lizano, S., 1987, ARA&A, 25, 23
Stapelfeldt, K.R., Krist, J.E., Menard, F., Bouvier, J., Padgett, D.L., & Burrows, C.J., 1998, ApJ, 502, L65
Sterzik, M., Pascucci, I., Apai, D., van der Bliek, N., & Dullemond, C. P. 2004, A&A, 427, 245
Walker, C., Wood, K., Lada, C. J., Robitaille, T., Bjorkman, J. E., & Whitney, B. 2004, MNRAS, 351, 607
Wood, K., Wolff, M.J., Bjorkman, J.E., & Whitney, B.A., 2002a, ApJ, 564, 887
Wood, K., Lada, C.J., Bjorkman, J.E., Kenyon, S.J., Whitney, B., & Wolff, M.J., 2002b, ApJ, 567, 1183